Inorganic Chemistry

Article

pubs.acs.org/IC

Metal–Organic Frameworks Based on Unprecedented Trinuclear and Pentanuclear Metal–Tetrazole Clusters as Secondary Building Units

Seok Jeong,[†,⊥] Xiaokai Song,[†,‡,⊥] Sehyun Jeong,[†] Minhak Oh,[†] Xinfang Liu,[†] Dongwook Kim,[†] Dohyun Moon,*[,§] and Myoung Soo Lah*[,†]

[†]Interdisciplinary School of Green Energy, Ulsan National Institute of Science & Technology, Ulsan, 689-798, Korea

[‡]Department of Chemistry and Applied Chemistry, Hanyang University, Ansan, Korea

[§]Pohang Accelerator Laboratory, Pohang, Korea

Supporting Information

ABSTRACT: Solvothermal reactions of manganese(II) chloride tetrahydrate with a bis-tetrazole ligand, 2,6-di(1*H*-tetrazol-5-yl)naphthalene (H_2NDT), in *N*,*N*′-dimethylformamide (DMF)/MeOH mixed solvent at two slightly different temperatures, 75 and 100 °C, led to two different metal–organic frameworks (MOFs), $[Mn^{II}_3O(HNDT)_2(NDT)(DMF)_3]$ (**1**) and $[Mn^{II}_5O_2(HNDT)_2(NDT)_2(DMF)_8]$ (**2**), with different net topologies. Single-crystal X-ray diffraction studies reveal that **1** is constructed from an unprecedented trinuclear building block, $[Mn^{II}_3O(CN_4)_6]$, as a 6-connected trigonal prismatic secondary building unit (SBU) of topological D_{3h} site symmetry, and that the ligand in the $HNDT^{-1}/NDT^{2-}$ deprotonation states is a linker, where two tetrazole (CN_4) groups of the ligand are connected via a rigid naphthyl group. The tetrazole groups in **1** adopt a 1,2-μ-bridging mode with the manganese(II) ions to form a μ^3-oxo trinuclear SBU. The trigonal prismatic SBU in **1** is connected to six neighboring SBUs to form a three-dimensional MOF of **acs** net topology. **2** is constructed from an unprecedented pentanuclear building block, $[Mn^{II}_5O_2(CN_4)_8]$, as an 8-connected tetragonal prismatic SBU of topological D_{4h} site symmetry. The tetrazole groups in **2** adopt monodentate, 1,2-μ- and 2,3-μ-bridging bidentate and 1,2,3-μ-bridging tridentate binding modes with the manganese(II) centers to form a bis-μ^3-oxo pentanuclear SBU of local C_2 site symmetry. The tetragonal prismatic SBU in **2** is connected to eight neighboring SBUs to form a 3-D MOF of **bcu** net topology.

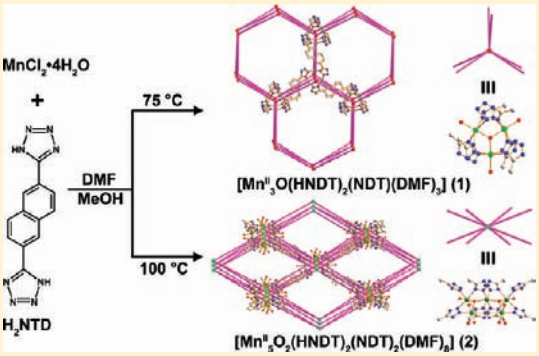

INTRODUCTION

Metal–organic frameworks (MOFs) have potential for use in diverse applications such as gas storage and separation, catalysis, and delivery.[1] Designing and predicting a MOF structure of a certain net topology from inorganic and organic building components are critical for the preparation of a MOF with the desired properties and characteristics. The network structures of MOFs are usually described as extended structures made of nodes and linkers.[2] Connectivity and symmetry of the inorganic and organic nodes and linkers probably play a key role in determining the framework structures of a certain specific net topology. Reticular MOFs can be obtained with the same secondary building unit (SBU) of specific connectivity and symmetry as a node.[3,4]

Synthesizing a new type of metal cluster as an SBU is important for developing a new MOF of a certain net topology. Ligands containing a tetrazole group can have diverse metal-binding modes using its four nitrogen donor atoms (Scheme 1),[5−13] and its metal clusters could be used as diverse SBUs of varying connectivity and symmetry (Scheme 2).[7a,9d,10a−c,g,11a,d,13a,e,14] Depending on the reaction conditions, including counteranions as potential auxiliary donors, MOFs of diverse net topologies could be obtained based on a 3-connected dinuclear cluster with a $M_2(CN_4)_3$ unit (where CN_4 represents the tetrazole group),[7a] 3-connected μ^3-oxo-bridged trinuclear cluster with a $M_3O(CN_4)_3$ unit,[14] 4-connected bis-μ-chloro-bridged linear trinuclear cluster with a $M_3Cl_2(CN_4)_4$ unit,[7a] 6-connected linear trinuclear cluster with a $M_3(CN_4)_6$ unit,[7a] 6-connected pentanuclear cluster with a $M_5(CN_4)_6$ unit,[11a] 6-connected hexanuclear cluster with a $M_6(CN_4)_6$ unit,[7a,9d,10c,g] 8-connected μ^4-chloro-bridged tetranuclear cluster with a $M_4Cl(CN_4)_8$ unit,[10a−c,13a] and a chloro-bridged linear chain[7a,10e,11d,13e] as SBUs.

In this study, we synthesized a bis-tetrazole ligand, 2,6-di(1*H*-tetrazol-5-yl)naphthalene (H_2NDT), containing a naphthyl group as a rigid linear residue connecting two tetrazole units. This ligand is similar to the well-known 1,4-benzeneditetrazol-5-yl (H_2BDT), which has a phenyl group as a connecting residue between two tetrazole units, except that it has a slightly longer naphthyl group as the connecting residue. The solvothermal reactions of H_2NDT with manganese(II) chloride tetrahydrate in *N*,*N*′-dimethylformamide (DMF)/MeOH

Received: August 28, 2011
Published: November 1, 2011

Scheme 1. Various Types of Tetrazole Binding Modes

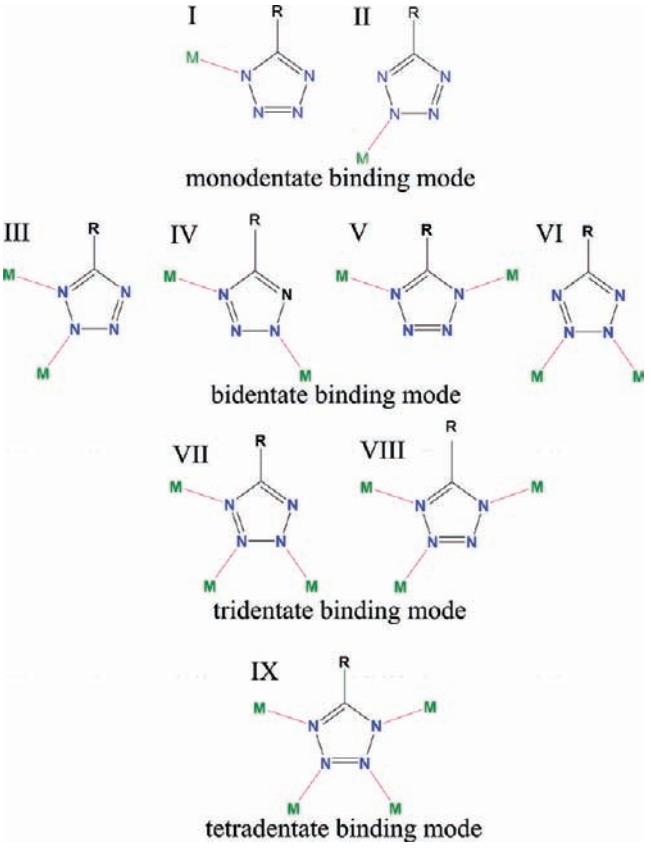

mixed solvent at two different temperatures, 75 and 100 °C, led to two topologically different MOFs based on two kinds of manganese tetrazole clusters, $[Mn_3O(CN_4)_6]$ and $[Mn_5O_2(CN_4)_8]$, as unprecedented 6-connected and 8-connected SBUs, respectively.

EXPERIMENTAL SECTION

General Procedures. All reagents were purchased from commercial sources and used without further purification. Elemental analyses were conducted on an elemental analyzer, Flash 2000, at the Ulsan National Institute of Science and Technology, Korea. Fourier Transform−Infrared (FT−IR) spectra were recorded as KBr pellets with a Varian 1000 FT−IR spectrophotometer (4000−400 cm^{-1}). Nuclear magnetic resonance (NMR) spectra were obtained on a Varian 600 NMR spectrometer. Powder X-ray diffraction (PXRD) data were recorded using a Rigaku D/M 2200T automated diffractometer at room temperature with a step size of 0.02° in 2θ angle. Simulated PXRD patterns were calculated with the Material Studio program[15] using single-crystal structures.

Preparation of H_2NDT. *Naphthalene-2,6-dicarboxamide.* A mixture of 2,6-naphthalenedicarboxylic acid (2.50 g, 11.6 mmol) and thionyl chloride (10.12 mL, 139.3 mmol) was stirred at 75 °C for 15 h. After removing the excess thionyl chloride under reduced pressure, the remaining solid was dissolved in 28 wt % aqueous ammonia (100 mL) at −20 °C (using an ice−salt bath). The reaction mixture was then warmed to room temperature. After being stirred for 12 h, the solid was collected by filtration and washed using distilled water (3 × 10 mL) and diethyl ether (3 × 10 mL). The product was dried at 120 °C for 12 h. Yield is 2.33 g, 93.8%. Elemental Analysis Calcd for $C_{12}H_{10}N_2O_2$ (fw =214.22): C, 67.28; H, 4.71; N, 13.08%. Found: C, 67.08; H, 4.73; N, 13.03%. ^{1}H NMR (dmso-d^6): δ 8.521 (s, 2H), 8.191 (s, 2H), 8.065 (d, 2H), 8.010 (d, 2H), 7.537 (s, 2H) ppm. ^{13}C NMR (dmso-d^6): δ 125.96, 127.44, 128.83, 133.00, 133.28, 167.73 ppm. IR (cm^{-1}, KBr pellet): 3354 (s), 3163 (s), 1652 (s), 1616 (s), 1500 (m), 1409 (s), 1366 (m), 1350 (m), 1195 (m), 1127 (m), 902 (s), 790 (s), 750 (s), 696 (m).

Scheme 2. Diverse Multinuclear Tetrazole Clusters as SBUs of Varying Connectivity and Symmetry

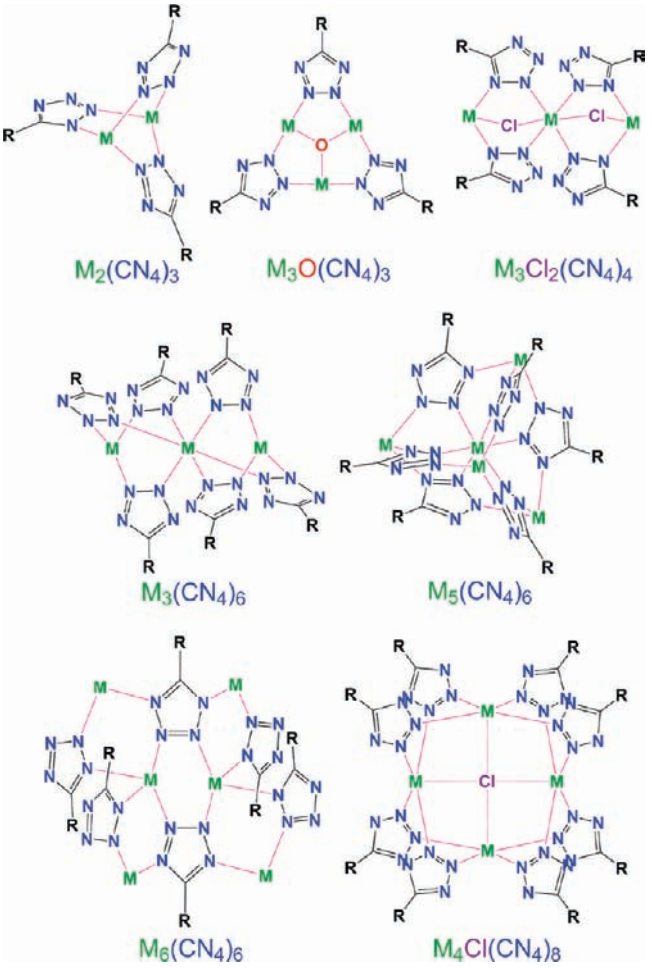

Naphthalene-2,6-dicarbonitrile. Naphthalene-2,6-dicarboxamide (2.25 g, 10.5 mmol) was stirred in 20 mL of *N,N′*-dimethylformamide (DMF), and 4.75 mL (65.4 mmol) of thionyl chloride was added to the suspension over 1 h while maintaining the temperature at 60 °C. The solution was stirred for 2 d at the same temperature until all the suspension was dissolved. The resulting solution was poured into 50 mL of 1 M HCl solution to decompose the excess thionyl chloride, giving a dense pale-gray precipitate. This solid was collected by filtration, and washed with distilled water until becoming neutral as monitored with pH paper. The filtrate was further washed using diethyl ether, and then dried at 120 °C for 12 h to afford 1.80 g (96.2%) of product. Elemental Analysis Calcd for $C_{12}H_6N_2$ (fw = 178.19): C, 80.89; H, 3.39; N, 15.72%. Found: C, 80.85; H, 3.36; N, 15.80%. ^{1}H NMR (dmso-d^6): δ 8.727 (s, 2H), 8.254 (d, 2H), 7.969 (d, 2H) ppm. ^{13}C NMR (dmso-d^6): δ 111.38, 118.45, 128.01, 129.94, 133.09, 134.36 ppm. IR (cm^{-1}, KBr pellet): 3079 (s), 3034 (s), 2226 (vs, C≡N), 1951 (m), 1882 (w), 1880 (s), 1657 (m), 1596 (s), 1488 (s), 1369 (s), 1344 (s), 1279 (s), 1208 (s), 1157 (m), 1136 (m), 980 (m), 902 (vs), 825 (vs), 662 (s).

H_2NDT. (***Caution!*** *H_2NDT must be handled carefully. It is known that several tetrazoles explode whey they are heated above their melting points.*) A mixture of naphthalene-2,6-dicarbonitrile (1.632 g, 9.159 mmol), NaN_3 (1.560 g, 24.00 mmol), and triethylamine hydrochloride (3.304 g, 24.00 mmol) in 20 mL of toluene/methanol mixed solvent (4:1 ratio) was refluxed for 4 d in a 250 mL round-bottom flask, and then cooled to room temperature. Thirty milliliters of 1 M NaOH solution was added to the mixture solution, and stirred for an

dx.doi.org/10.1021/ic201883f | *Inorg. Chem.* 2011, 50, 12133–12140

Table 1. Crystal Data and Structure Refinements for 1 and 2

	1	2
empirical formula	$C_{45}H_{41}N_{27}O_4Mn_3$	$C_{72}H_{82}N_{40}O_{10}Mn_5$
formula weight	1188.87	1942.48
temperature (K)	143(2)	153(2)
wavelength (Å)	0.71073	0.75000
crystal system	hexagonal	monoclinic
space group	$P6_3/m$	$C2/c$
unit cell dimensions (Å and deg)	a = 20.792(4)	a = 36.795(7)
	b = 20.792(4)	b = 15.904(3)
	c = 13.814(3)	c = 26.761(5)
	α = 90	α = 90
	β = 90	β = 131.73(3)
	γ = 120	γ = 90
volume (Å^3)	5172(2)	11688(4)
Z	2	4
density (calculated) (Mg/m^3)	0.763	1.104
absorption coefficient (mm^{-1})	0.397	0.585
F(000)	1214	3996
crystal size (mm^3)	0.50 × 0.40 × 0.35	0.35 × 0.22 × 0.11
reflections collected	27598	51411
independent reflections	4410 [R(int) = 0.0865]	14503 [R(int) = 0.0901]
completeness (%)	96.9 (θ = 28.48°)	99.9 (θ = 30.00°)
goodness-of-fit on F^2	1.029	1.097
final R indices [$I > 2\sigma(I)$]	R1 = 0.0629	R1 = 0.0816
	wR2 = 0.1368	wR2 = 0.2472
R indices (all data)	R1 = 0.0943	R1 = 0.0932
	wR2 = 0.1488	wR2 = 0.2598
largest diff. peak and hole (e·Å^{-3})	0.743 and −0.667	1.355 and −1.504

additional 2 h. The aqueous layer was treated with about 30 mL of 1 M aqueous HCl solution until no further precipitate formed. The precipitate was collected by filtration, dried in air, and dissolved in 50 mL of an aqueous NaOH solution (1 M). When the solution became clear, the brown-colored solution was titrated with about 50 mL of aqueous HCl (1 M) solution until the pH of the solution was ~7. The precipitate was washed with successive aliquots of distilled water (3 × 50 mL) and diethyl ether (2 × 30 mL) and dried in air to afford 1.700 g (70.24%) of product. Elemental Analysis Calcd for $C_{12}H_8N_8$ (fw = 264.25): C, 54.54; H, 3.05; N, 42.40%. Found: C, 54.52; H, 3.13; N, 42.74%. ^{1}H NMR (dmso-d^6): δ 8.770 (s, 2H), 8.297 (d, 2H), 8.240 (d, 2H) ppm. ^{13}C NMR (dmso-d^6): δ 123.34, 124.85, 126.84, 130.03, 133.47, 155.66 ppm. IR (cm^{-1}, KBr pellet): 3562 (s), 3377 (s), 3218 (m), 2948 (w), 2879 (w), 1633 (s), 1559 (w), 1475 (s), 1387 (s), 1359 (m), 1307 (m), 1186 (s), 1121 (w), 1025 (w), 965 (w), 899 (s), 880 (m), 811 (s), 759 (s), 665 (w).

Preparation of MOFs. *$[Mn_3O(HNDT)_2(NDT)(DMF)_3]\cdot 3DMF\cdot 15H_2O$,* ***1.*** A solution of $MnCl_2\cdot 4H_2O$ (29.7 mg, 0.150 mmol) in 0.5 mL of methanol was added to a 2.0 mL DMF solution of H_2NDT (13.2 mg, 0.050 mmol). The 2.5 mL solution was poured into a 4 mL vial and heated at 75 °C for 4 d. Block-shaped pale-brown single crystals were obtained and washed using DMF, and then dried in air to afford a total of 21.0 mg of a crystalline product (75.1%, based on ligand). Elemental Analysis Calcd for $[Mn_3O(C_{12}H_6N_8)_3(C_3H_7NO)_3 + 2H^+]\cdot 3C_3H_7NO\cdot 15H_2O$ (fw = 1678.33): C, 38.65; H, 5.53; N, 25.04%. Found: C, 38.44; H, 5.40; N, 24.88%. IR (cm^{-1}, KBr pellet): 3200 (s), 2882 (w), 2830 (w), 1666 (s, DMF C═O stretching), 1470 (s), 1436 (w), 1382 (s), 1309 (w), 1249 (w), 1184 (m), 1151 (w), 1102 (s), 1027 (w), 909 (s), 880 (s), 767 (s), 729 (w), 669 (m).

$[Mn_5O_2(HNDT)_2(NDT)_2(DMF)_8]\cdot 2DMF\cdot 5H_2O$, ***2.*** **2** was prepared according to the same synthetic procedure for **1** but the solution was heated at 100 °C for 4 h. Flake-shaped pale-brown single crystals were obtained and washed using DMF, and then dried in air to afford a total of 18.1 mg of a crystalline product (66.5%, based on ligand). Elemental Analysis Calcd for $[Mn_5O_2(C_{12}H_6N_8)_4(C_3H_7NO)_8 + 2H^+]\cdot 2C_3H_7NO\cdot 5H_2O$ (fw = 2178.66): C, 43.00; H, 4.90; N, 27.00%. Found: C, 43.03; H, 4.87; N, 26.62%. IR (cm^{-1}, KBr pellet): 2935 (w), 1672 (s, C═O stretching of lattice DMF), 1648 (vs, C═O stretching of ligated DMF), 1603 (s), 1500 (w), 1468 (m), 1384 (s), 1345 (s), 1255 (m), 1179 (m), 1140 (w), 1111 (s), 1061 (w), 1023 (w), 909 (m), 878 (m), 835 (m), 767 (s), 683 (s).

Crystallographic Data Collection and Refinement of Structures. *Crystal Structure Determination for $Mn_3O(HNDT)_2(NDT)(DMF)_3$,* ***1.*** The diffraction data for a crystal coated with paratone oil were measured at 143 K with Mo Kα radiation on a Bruker SMART CCD equipped with a graphite-crystal, incident-beam monochromator. The SMART and SAINT software packages[16] were used for data collection and integration, respectively. The collected data were corrected for absorbance using SADABS[17] based upon Laue symmetry using equivalent reflections. Structures were solved by direct methods and refined by full-matrix least-squares calculations with the SHELXTL-PLUS (ver. 5.1) software package.[18] A ligand on a crystallographic inversion center, a manganese ion and a ligated DMF on the crystallographic mirror plane, and a μ^3-oxo oxygen atom of the Mn_3O cluster unit on the crystallographic −6 symmetry site were found as an asymmetric unit. Three partially identified solvent sites were also found in the difference Fourier map. All nonhydrogen atoms were refined anisotropically except the lattice solvent molecules; hydrogen atoms were assigned isotropic displacement coefficients (U(H) = 1.2U(C)), and their coordinates were allowed to ride on their respective atoms. The hydrogen atoms of the tetrazole unit of the ligand, the methyl groups of the ligated DMF molecule, and the lattice solvent molecules were not included in the least-squares refinement. The refinement converged to $R1$ = 0.1377, and $wR2$ = 0.3385 for 3487 reflections of $I > 2\sigma(I)$. Structure refinement after modification of the data for the noncoordinate lattice solvent molecules with the SQUEEZE routine of PLATON (3057 Å^3, 59.0% of the crystal volume, 1032 solvent electrons [~26 DMF molecules] per unit cell)[19] led to better refinement and data convergence. Refinement of the

dx.doi.org/10.1021/ic201883f | Inorg. Chem. 2011, 50, 12133–12140

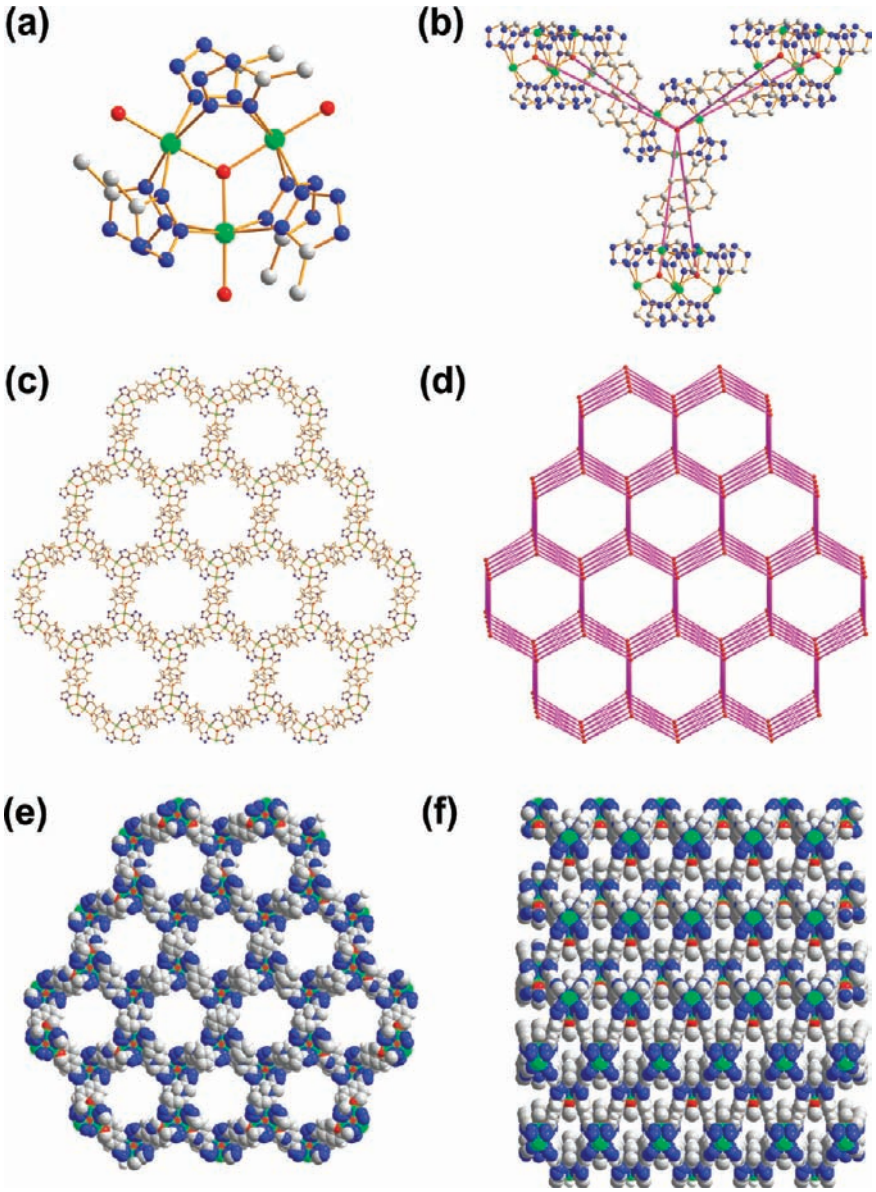

Figure 1. Network structure of **1** with **acs** net topology. (a) $Mn_3O(CN_4)_6(DMF)_3$ cluster as a 6-connected SBU of local C_{3h} site symmetry. (b) Ball-and-stick diagram of a central 6-connected node of topological D_{3h} site symmetry surrounded by six SBUs, where the red balls represent the 6-connected nodes and the purple sticks represent the connectivity between the nodes. (c) Ball-and-stick packing diagram of **1** viewed along the crystallographic *c*-axis. (d) Schematic diagram of **1** with **acs** net topology viewed along the approximate crystallographic *c*-axis. (e) Space-filling packing diagram of **1** viewed along the crystallographic *c*-axis. (f) Space-filling packing diagram of **1** viewed along the crystallographic *b*-axis.

structure converged to a final *R1* = 0.0629, and *wR2* = 0.1368 for 3244 reflections of $I > 2\sigma(I)$; *R1* = 0.0943, and *wR2* = 0.1488 for all reflections. Crystal and intensity data are given in Table 1.

Crystal Structure Determination for $Mn_5O_2(HNDT)_2(NDT)_2(DMF)_8$ **2**. A single crystal of **2** was coated with paratone oil. The diffraction data were measured at 153 K with synchrotron radiation (λ = 0.75000 Å) on a 6B MX-I ADSC Quantum-210 detector with a silicon (111) double-crystal monochromator at the Pohang Accelerator Laboratory, Korea. The ADSC Quantum-210 ADX program (Ver. 1.92)[20] was used for data collection, and HKL2000 (Ver. 0.98.699)[21] was used for cell refinement, reduction, and absorption correction. The crystal structure of **2** was solved by a direct method and refined by full-matrix least-squares calculation with the SHELXTL-Plus (Ver. 5.1) software package.[18] Two ligands, three manganese ions including one on a crystallographic 2-fold axis, four ligated DMF molecules including two statistically disordered ones, two lattice DMF molecules including one statistically disordered one, and four partially occupied lattice water sites (some of them could be partially identified methanol or DMF molecules) were found as an asymmetric unit. All nonhydrogen atoms were refined anisotropically except two lattice water molecules; hydrogen atoms were assigned isotropic displacement coefficients (U(H) = 1.2U(C) or 1.5U(C_{methyl})), and their coordinates were allowed to ride on their respective atoms. The hydrogen atoms of the tetrazole unit of the ligand and the lattice water molecules were not included in the least-squares refinement. The refinement of the model converged to *R1* = 0.2078 and *wR2* = 0.4870 for 15379 reflections of $I > 2\sigma(I)$. Structure refinement after modification of the data for the lattice solvent sites with the SQUEEZE routine of PLATON (3524 Å^3, 30.2% of the crystal volume, 364 solvent electrons [~10 DMF molecules] per unit cell)[19] led to better refinement and data convergence. Refinement converged to a final *R1* = 0.0816 and *wR2* = 0.2472 for 10897 reflections of $I > 2\sigma(I)$; *R1* = 0.0932 and *wR2* = 0.2598 for all reflections. Crystal and intensity data are given in Table 1.

Low-Pressure Gas Sorption Measurements. All gas sorption isotherms were measured using a BELSORP-max (BEL Japan, Inc.)

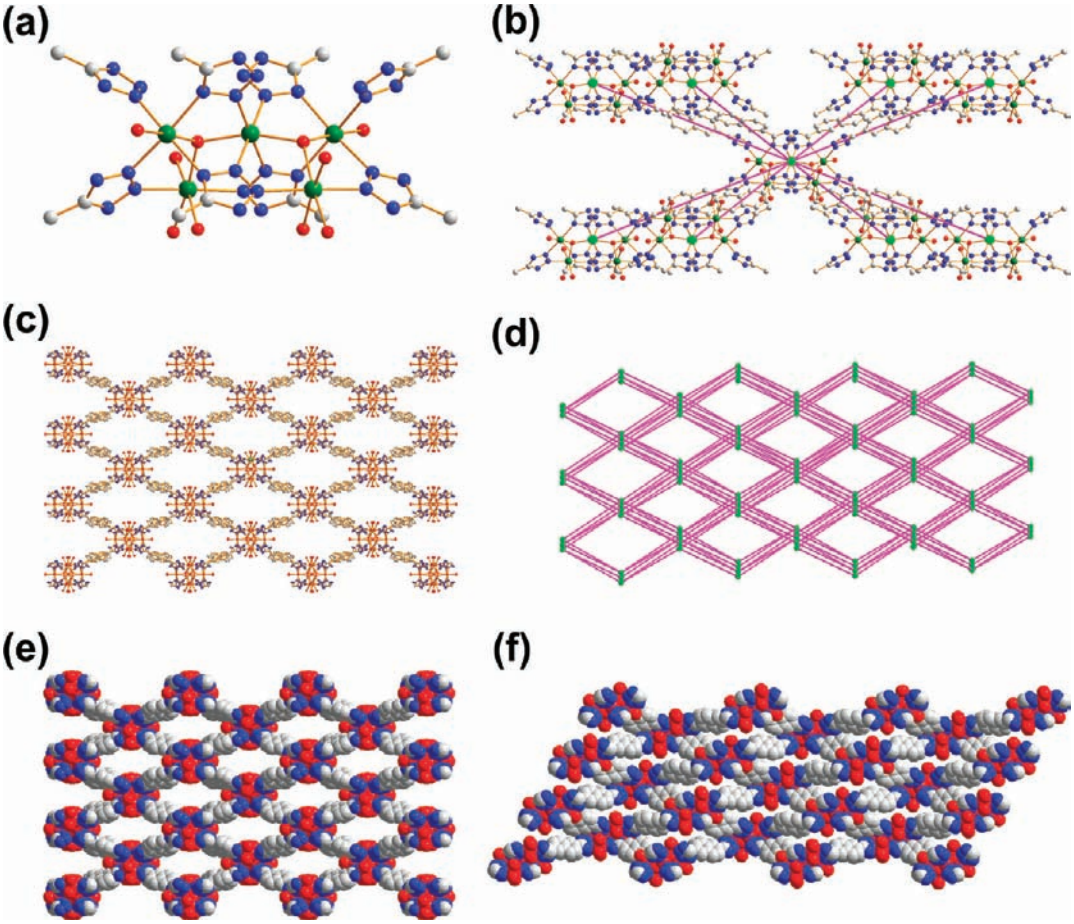

Figure 2. Network structure of **2** with **bcu** net topology. (a) $Mn_5O_2(CN_4)_8(solvent)_8$ cluster as an 8-connected SBU of local C_2 site symmetry. (b) Ball-and-stick diagram of a central 8-connected node of topological D_{4h} site symmetry surrounded by eight SBUs, where the bright green balls represent the 6-connected nodes and the purple sticks represent the connectivity between the nodes. (c) Ball-and-stick packing diagram of **2** viewed along the crystallographic *c*-axis. (d) Schematic diagram of **2** with **bcu** net topology viewed along the approximate crystallographic *c*-axis. (e) Space-filling packing diagram of **2** viewed along the crystallographic *c*-axis. (f) Space-filling packing diagram of **2** viewed along the crystallographic *b*-axis.

with a standard volumetric technique up to saturated pressure. The N_2 (with purity of 99.999%) sorption isotherms were monitored at 77 K. The adsorption data in the pressure range lower than ~0.1 P/P_0 were fitted to the Brunauer–Emmett–Teller (BET) equation to determine the BET surface areas. For the Langmuir surface areas, data from the whole adsorption data were used. The H_2 (99.999%) sorption isotherms were measured at both 77 and 87 K; the CO_2 (99.99%) and CH_4 (99.99%) sorption isotherms were measured at 195 K.

RESULTS AND DISCUSSION

A solvothermal reaction of H_2NDT with $Mn(II)Cl_2{\cdot}4H_2O$ in DMF/methanol mixed solvent at 75 °C afforded pale-brown rectangular crystals of $Mn_3O(HNDT)_2(NDT)(DMF)_3$, **1** (Figure 1). The μ^3-oxo bridged three manganese ions with six 1,2-bridged tetrazole groups (type III binding mode in Scheme 1) of the ligand to form a $[Mn^{II}{}_3O(CN_4)_6]$ SBU of local C_{3h} site symmetry (Figure 1a). The SBU is structurally similar to the well-known $[M_3O(COO)_6]$ SBU (M = Cr(III), Fe(III), Al(III))[22,23] but the oxidation state of the manganese ion is +2. There is no indication of counteranionic species in the difference Fourier map of the single-crystal structure or from the elemental analysis. Matching a structural model with no counteranionic species suggests that two-thirds of the tetrazole units of the ligands in the network are protonated for charge balance. Although the local site symmetry of the $[Mn^{II}{}_3O(CN_4)_6]$ SBU with six 1,2-bridged tetrazole groups is C_{3h}, the topological site symmetry of the SBU is trigonal prismatic D_{3h} (Figure 1b, 1d). The topological trigonal prismatic 6-connected $[Mn^{II}{}_3O(CN_4)_6]$ SBUs in **1** are interconnected via the naphthyl group of the ligand with a network of a uninodal **acs** net topology (Figure 1c, 1d). Although **acs** net is a semiregular net, only a few examples of MOFs of **acs** net topology with a trigonal prismatic 6-connected node have been reported.[24] The network of the **acs** net topology with ~60 vol % lattice solvent pores has one-dimensional (1-D) cylindrical channels of ~1.2 nm in diameter along the crystallographic *c*-axis (Figure 1e) and the 1-D channels are interconnected with a three-dimensional (3-D) microporous network structure (Figure 1f).

The same solvothermal reaction of H_2NDT with $Mn(II)Cl_2{\cdot}4H_2O$ in DMF/methanol mixed solvent but at 100 °C afforded pale-brown flake-shaped crystals of $Mn_5O_2(HNDT)_2(NDT)_2(DMF)_8$, **2** (Figure 2). A pentanuclear manganese cluster, $[Mn^{II}{}_5O_2(CN_4)_8]$ unit, is made of corner-shared two μ^3-oxo-bridged Mn_3O units with six tetrazole groups in three different bridging modes (types III, VI, and VII) and two additional tetrazole groups in a monodentate binding mode (type II). The 8-connected pentanuclear manganese cluster serves as a C_2 site symmetric SBU (Figure 2a). The SBUs serving as a topological tetragonal prismatic 8-connected node (Figure 2b, 2d) are interconnected with a network of **bcu** net topology (Figure 2c, 2d). Although **bcu** net is a textbook

dx.doi.org/10.1021/ic201883f | *Inorg. Chem.* 2011, 50, 12133–12140

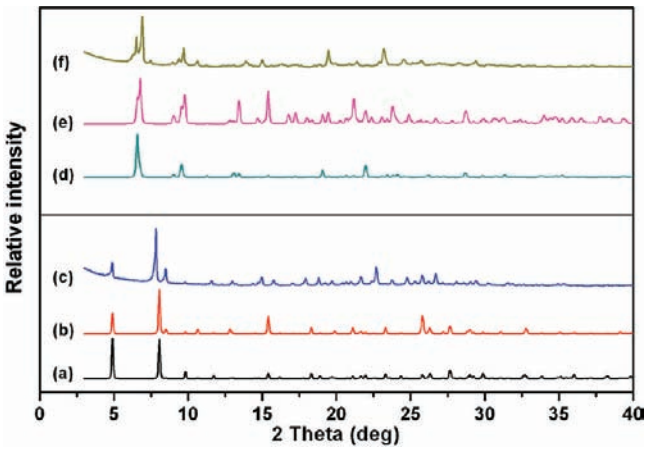

Figure 3. PXRD patterns of **1** and **2**. (a) A simulated PXRD pattern from a single-crystal structure model of **1**. (b) A simulated PXRD pattern of **1** with (0 1 0) preferred orientation. (c) A PXRD pattern of as-synthesized sample of **1**. (d) A simulated PXRD pattern from a single-crystal structure model of **2**. (e) A simulated PXRD pattern of **2** with (0 2 1) preferred orientation. (f) A PXRD pattern of as-synthesized sample of **2**.

example of one of five regular nets, MOFs of **bcu** net topology with an 8-connected node have only appeared in a few examples.[25] The network of **2** with ~30 vol % lattice solvent pores also has 1-D channels along the crystallographic *c*-axis partially packed with the flexible ligated solvent DMF molecules (Figure 2e, 2f).

The PXRD patterns of as-synthesized **1** and **2** show that the single crystals of **1** and **2** are representatives of the corresponding bulk samples, respectively (Figure 3).

Sorption Behaviors. The activated sample **1a** was prepared by keeping as-synthesized **1** in fresh DMF for 3 d, and then the DMF was exchanged with methanol by gradually replacing a small portion of the (mixed) solvent with methanol until a final purely methanol solvent was achieved. The soaking solvent of the sample was decanted and freshly replenished using dichloromethane several times, after which the sample was vacuum-dried at 80 °C for 1 d. The N_2 sorption isotherm of **1a** shows a typical type I adsorption isotherm at 77 K, and 1 atm (Figure 4a). The amount of N_2 adsorbed is ~433 $cm^3\ g^{-1}$ at ~1 P/P_0 and the BET and Langmuir surface areas are 1400 $m^2\ g^{-1}$ and 1810 $m^2\ g^{-1}$, respectively. Noticeably, the specific pore volume occupied by N_2, 0.669 $cm^3\ g^{-1}$,[26] is slightly less than the specific pore volume calculated from the single-crystal structure of **1**, 0.773 $cm^3\ g^{-1}$ (Table 2), which reflects partial defectiveness in the pore structure of the sample that either originated from the as-synthesized sample or was generated during the activation process.

The amounts of adsorbed CO_2 and CH_4 on **1a** at 195 K and 1 bar are 362 $cm^3\ g^{-1}$ (542 g L^{-1}) and 94 $cm^3\ g^{-1}$ (51 g L^{-1}), respectively (Figure 4b). The amount of hydrogen uptake on **1a** is 1.2 wt % at 77 K and 1 bar, which is within the range expected based on the specific surface area (Figure 4c).[27] The isosteric heat of adsorption calculated from the H_2 isotherms at 77 and 87 K using the virial method[28] is in the range of 6.8−5.7 kJ mol^{-1} for **1a** (coverage of 0.005−0.8 wt % H_2 uptake) depending on the degree of H_2 loading (Figure 4d). Despite the lack of so-called unsaturated metal sites for effective adsorbent−adsorbate interaction, the relatively high isosteric heats of H_2 adsorption might be related to the high content of electronegative nitrogen atoms in the ligand.

Although the activated samples of **2** were prepared using several different activation procedures including the procedure employed for sample **1a**, none of them showed N_2 sorption behavior (**2a** is shown in Figure 4a as an example). The

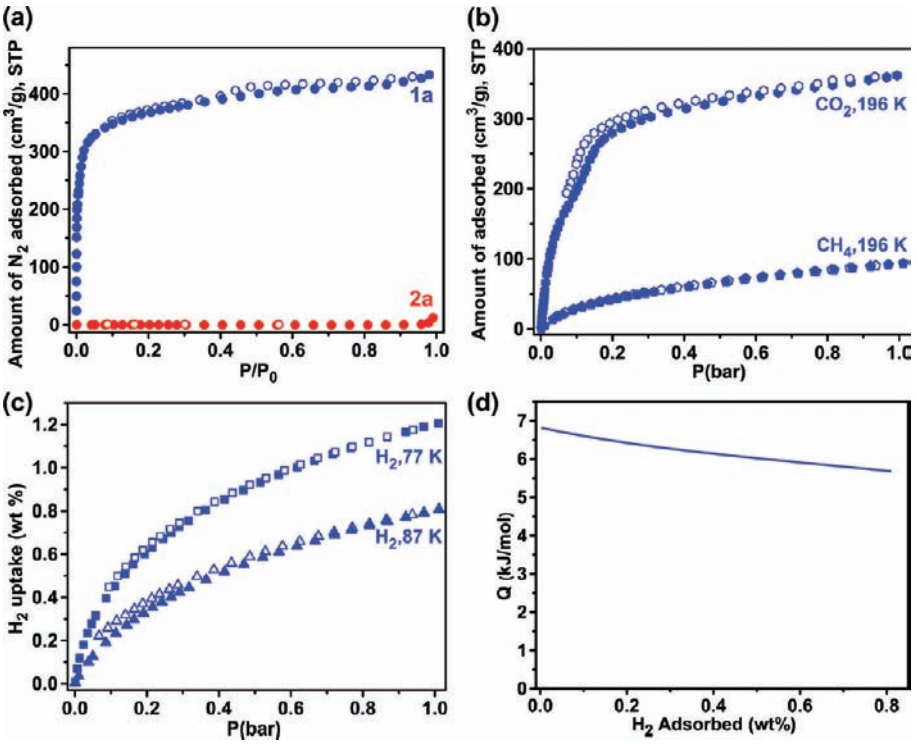

Figure 4. Gas sorption isotherms on **1a** (blue symbols) and **2a** (red symbols), where filled symbols represent adsorption isotherms and open symbols represent desorption isotherms. (a) N_2 sorption isotherms on **1a** and **2a** at 77 K. (b) CO_2 and CH_4 sorption isotherms on **1a** at 196 K. (c) H_2 sorption isotherms on **1a** at 77 and 87 K. (d) H_2 adsorption enthalpy on **1a**.

dx.doi.org/10.1021/ic201883f | *Inorg. Chem.* 2011, 50, 12133–12140

activation process of **2** with eight ligated solvent molecules per pentanuclear cluster probably leads to collapse of the pore structure.

CONCLUSIONS

The tetrazole unit of the ligand in the $HNDT^{-1}/NDT^{2-}$ deprotonation states with four possible donor nitrogen atoms of diverse coordination modes offers very rich coordination chemistry. The same solvothermal reactions of a bis-tetrazole ligand, H_2NDT, with manganese(II) chloride tetrahydrate in DMF/MeOH mixed solvent but at two slightly different temperatures led to two MOFs, **1** and **2**, of different net topologies with two unprecedented $Mn_3O(CN_4)_6$ and $Mn_5O_2(CN_4)_8$ clusters as 6- and 8-connected SBUs, respectively. While the reaction at 75 °C generated **1**, $Mn_3O(HNDT)_2(NDT)(DMF)_3$, of **acs** net topology using a $[Mn_3O(CN_4)_6]$ cluster as a topological D_{3h} symmetric 6-connected SBU with three additional ligated solvent molecules, the reaction at 100 °C generated **2**, $Mn_5O_2(HNDT)_2(NDT)_2(DMF)_8$, of **bcu** net topology using a $[Mn_5O_2(CN_4)_8]$ cluster as a topological D_{4h} symmetric 8-connected SBU with eight additional ligated solvent molecules. Corner-sharing of a manganese atom of the two 6-connected trinuclear units, $[Mn_3O(CN_4)_6(DMF)_3]$, in **1** resulted in the C_2 symmetric 8-connected pentanuclear unit, $[Mn_5O_2(CN_4)_8(DMF)_8]$, in **2**. The reaction at the increased temperature merged the two trinuclear units in **1** into a single pentanuclear unit in **2**.

While the gas sorption behaviors of the activated sample **1a** indicate that it is microporous, we could not find any proper activation condition for **2** probably because of the instability of the framework. Although the approximate solvent pore volume of **2** was about half that of **1**, the larger number of ligated solvent molecules of the SBU in **2** than in **1** might be responsible for the framework instability.

ASSOCIATED CONTENT

Supporting Information

X-ray crystallographic files (CIF) for **1** and **2**. This material is available free of charge via the Internet at http://pubs.acs.org.

AUTHOR INFORMATION

Corresponding Author

*Phone: 82-52-217-2931 (M.S.L.). Fax: 82-52-217-2019 (M.S.L.). E-mail: mslah@unist.ac.kr (M.S.L.).

Author Contributions

⊥These authors contributed equally to this article.

ACKNOWLEDGMENTS

This work was supported by NRF-2010-0019408 and WCU programs (R31-2008-000-20012-0) through the National Research Foundation of Korea. The authors acknowledge PAL for beamline use (2010-2063-08).

REFERENCES

(1) (a) Ma, S.; Zhou, H.-C. *Chem. Commun.* **2010**, *46*, 44. (b) Murray, L. J.; Dincă, M.; Long, J. R. *Chem. Soc. Rev.* **2009**, *38*, 1294. (c) Li, J.-R.; Kuppler, R. J.; Zhou, H.-C. *Chem. Soc. Rev.* **2009**, *38*, 1477. (d) Férey, G. *Chem. Soc. Rev.* **2008**, *37*, 191. (e) Horcajada, P.; Chalati, T.; Serre, C.; Gillet, B.; Sebrie, C.; Baati, T.; Eubank, J. F.; Heurtaux, D.; Clayette, P.; Kreuz, C.; Chang, J.-S.; Hwang, Y. K.; Marsaud, V.; Bories, P.-N.; Cynober, L.; Gil, S.; Férey, G.; Couvreur, P.; Gref, R. *Nat. Mater.* **2010**, *9*, 172. (f) Lee, J. Y.; Farha, O. K.; Roberts, J.; Scheidt, K. A.; Nguyen, S. B. T.; Hupp, J. T. *Chem. Soc. Rev.* **2009**, *38*, 1450. (g) Ma, L.; Abney, C.; Lin, W. *Chem. Soc. Rev.* **2009**, *38*, 1248.

(2) (a) O'Keeffe, M.; Eddaoudi, M.; Li, H.; Reineke, T.; Yaghi, O. M. *J. Solid State Chem.* **2000**, *152*, 3. (b) O'Keeffe, M. *Chem. Soc. Rev.* **2009**, *38*, 1215.

(3) (a) Li, H.; Eddaoudi, M.; O'Keeffe, M.; Yaghi, O. M. *Nature* **1999**, *402*, 276. (b) Eddaoudi, M.; Kim, J.; Rosi, N.; Vodak, D.; Wachter, J.; O'Keeffe, M.; Yaghi, O. M. *Science* **2002**, *295*, 469. (c) Yaghi, O. M.; O'Keeffe, M.; Ockwig, N. W.; Chae, H. K.; Eddaoudi, M.; Kim, J. *Nature* **2003**, *423*, 705. (d) Rosi, N. L.; Eckert, J.; Eddaoudi, M.; Vodak, D. T.; Kim, J.; O'Keeffe, M.; Yaghi, O. M. *Science* **2003**, *300*, 1127.

(4) (a) Chui, S. S.-Y.; Lo, S. M.-F.; Charmant, J. P. H.; Orpen, A. G.; Williams, I. D. *Science* **1999**, *283*, 1148. (b) Wang, X.-S.; Ma, S.; Sun, D.; Parkin, S.; Zhou, H.-C. *J. Am. Chem. Soc.* **2006**, *128*, 16474. (c) Ma, S.; Sun, D.; Ambrogio, M.; Fillinger, J. A.; Parkin, S.; Zhou, H.-C. *J. Am. Chem. Soc.* **2007**, *129*, 1858. (d) Wang, X.-S.; Ma, S.; Yuan, D.; Yoon, J. W.; Hwang, Y. K.; Chang, J.-S.; Wang, X.; Jørgensen, M. R.; Chen, Y.-S.; Zhou, H.-C. *Inorg. Chem.* **2009**, *48*, 7519.

(5) Wang, Y.-C.; Zhao, H.; Song, Y.-M.; Wang, X.-S.; Xiong, R.-G. *Appl. Organomet. Chem.* **2004**, *18*, 494.

(6) (a) Kostakis, G. E.; Abbas, G.; Anson, C. E.; Powell, A. K. *CrystEngComm* **2009**, *11*, 82. (b) Hill, M.; Mahon, M. F.; McGinley, J.; Molloy, K. C. *J. Chem. Soc., Dalton Trans.* **1996**, 835.

(7) (a) Dincă, M.; Yu, A. F.; Long, J. R. *J. Am. Chem. Soc.* **2006**, *128*, 8904. (b) Huang, X.-H.; Sheng, T.-L.; Xiang, S.-C.; Fu, R.-B.; Hu, S.-M.; Li, Y.-M.; Wu, X.-T. *Inorg. Chem. Commun.* **2006**, *9*, 1304.

(8) (a) Hill, M.; Mahon, M. F.; Molloy, K. C. *J. Chem. Soc., Dalton Trans.* **1996**, 1857. (b) Jiang, T.; Zhao, Y.-F.; Zhang, X.-M. *Inorg. Chem. Commun.* **2007**, *10*, 1194.

(9) (a) Li, J.-R.; Tao, Y.; Yu, Q.; Bu, X.-H. *Chem. Commun.* **2007**, 1527. (b) Ye, Q.; Li, Y.-H.; Song, Y.-M.; Huang, X.-F.; Xiong, R.-G.; Xue, Z. *Inorg. Chem.* **2005**, *44*, 3618. (c) Wang, X.-S.; Tang, Y.-Z.; Huang, X.-F.; Qu, Z.-R.; Che, C.-M.; Chan, P. W. H.; Xiong, R.-G. *Inorg. Chem.* **2005**, *44*, 5278. (d) Jiang, C.; Yu, Z.; Jiao, C.; Wang, S.; Li, J.; Wang, h.; Cui, Y. *Eur. J. Inorg. Chem.* **2004**, 4669.

(10) (a) Dincă, M.; Han, W. S.; Liu, Y.; Dailly, A.; Brown, C. M.; Long, J. R. *Angew. Chem., Int. Ed.* **2007**, *46*, 1419. (b) Dincă, M.; Dailly, A.; Liu, Y.; Brown, C. M.; Neumann, D. A.; Long, J. R. *J. Am. Chem. Soc.* **2006**, *128*, 16876. (c) Dincă, M.; Dailly, A.; Long, J. R. *Chem.—Eur. J.* **2008**, *14*, 10280. (d) Nouar, F.; Eubank, J. F.; Bousquet, T.; Wojtas, L.; Zaworotko, M. J.; Eddaoudi, M. *J. Am. Chem. Soc.* **2008**, *130*, 1833. (e) Ouellette, W.; Prosvirin, A. V.; Whitenack, K.; Dunbar, K. R.; Zubieta, J. *Angew. Chem., Int. Ed.* **2009**, *48*, 2140. (f) Ye, Q.; Song, Y.-M.; Wang, G.-X.; Chen, K.; Fu, D.-W.; Chan, P. W. H.; Zhu, J.-S.; Huang, S. D.; Xiong, R.-G. *J. Am. Chem.* **2006**, *128*, 6554. (g) Tao, J.; Ma, Z.-J.; Huang, R.-B.; Zheng, L.-S. *Inorg. Chem.* **2004**, *43*, 6133. (h) Ye, Q.; Song, Y.-M.; Fu, D.-W.; Wang, G.-X.; Xiong, R.-G.; Chan, P. W. H.; Huang, S. D. *Cryst. Growth Des.* **2007**, *7*, 1568.

(11) (a) Wang, X.-S.; Tang, Y.-Z.; Huang, X.-F.; Qu, Z.-R.; Che, C.-M.; Chan, P. W. H.; Xiong, R.-G. *Inorg. Chem.* **2005**, *44*, 5278. (b) Bhandari, S.; Mahon, M. F.; Molloy, K. C.; Palmer, J. S.; Sayers, S. F. *J. Chem. Soc., Dalton Trans.* **2000**, 1053. (c) Ding, Y.-B.; Cheng, Y.; Zhang, Z.-L.; Zhang, J.; Yin, Y.-G.; Gao, W.-H. *Inorg. Chem. Commun.* **2009**, *12*, 45. (d) Chen, Y.; Ren, Z.-G.; Li, H.-X.; Tang, X.-Y.; Zhang, W.-H.; Zhang, Y.; Lang, J.-P. *J. Mol. Struct.* **2008**, *875*, 339.

(12) Yu, Z.; Xie, Y.; Wang, S.; Yong, G.; Wang, Z. *Inorg. Chem. Commun.* **2008**, *11*, 372.

(13) (a) Dincă, M.; Dailly, A.; Tsay, C.; Long, J. R. *Inorg. Chem.* **2008**, *47*, 11. (b) Wu, T.; Yi, B.-H.; Li, D. *Inorg. Chem.* **2005**, *44*, 4130. (c) Li, M.; Li, Z.; Li, D. *Chem. Commun.* **2008**, 3390. (d) Zhang, X.-M.; Zhao, Y.-F.; Wu, H.-S.; Batten, S. R.; Ng, S. W. *Dalton Trans.* **2006**, 3170. (e) Wu, T.; Chen, M.; Li, D. *Eur. J. Inorg. Chem.* **2006**, 2132.

(14) Deng, H.; Qiu, Y.-C.; Li, Y.-H.; Liu, Z.-H.; Zeng, R.-H.; Zellerb, M.; Batten, S. R. *Chem. Commun.* **2008**, 2239.

(15) *Materials Studio program*, version 4.3; Accelrys: San Diego, CA, 2008.

(16) *SMART and SAINT, Area Detector Software Package and SAX Area detector Integration Program*; Bruker Analytical X-ray: Madison, WI, 1997.
(17) *SADABS, Area Detector Absorption Correction Program*; Bruker Analytical X-ray: Madison, WI, 1997.
(18) *SHELX program*: Sheldrick, G. M. *Acta Crystallogr., Sect. A* **2008**, *64*, 112.
(19) *PLATON program*: Spek, A. L. *Acta Crystallogr., Sect. A* **1990**, *46*, 194.
(20) Arvai, A. J.; Nielsen, C. *ADSC Quantum-210 ADX Program*; Area Detector System Corporation: Poway, CA, 1983.
(21) Otwinowski, Z.; Minor, W. In *Methods in Enzymology*; Carter, C. W., Jr.; Sweet, R. M. Academic Press: New York, 1997; p 276, part A, pp 307−326.
(22) (a) Férey, G.; Serre, C.; Mellot-Draznieks, C.; Millange, F.; Surblé, S.; Dutour, J.; Margiolaki, I. *Angew. Chem., Int. Ed.* **2004**, *43*, 6296. (b) Küsgens, P.; Rose, M.; Senkovska, I.; Fröde, H.; Henschel, A.; Siegle, S.; Kaskel, S. *Microporous Mesoporous Mater.* **2009**, *120*, 325. (c) Volkringer, C.; Popov, D.; Loiseau, T.; Férey, G.; Burghammer, M.; Riekel, C.; Haouas, M.; Taulelle, F. *Chem. Mater.* **2009**, *21*, 5695.
(23) (a) Férey, G.; Mellot-Draznieks, C.; Serre, C.; Millange, F.; Dutour, J.; Surblé, S.; Margiolaki, I. *Science* **2005**, *309*, 2040. (b) Bauer, S.; Serre, C.; Devic, T.; Horcajada, P.; Marrot, J.; Férey, G.; Stock, N. *Inorg. Chem.* **2008**, *47*, 7568. (c) Serra-Crespo, P.; Ramos-Fernandez, E. V.; Gascon, J.; Kapteijn, F. *Chem. Mater.* **2011**, *23*, 2565.
(24) (a) Friedrichs, O. D.; O'Keeffe, M.; Yaghi, O. M. *Acta Crystallogr.* **2003**, *A59*, 515. (b) Devic, T.; Serre, C.; Audebrand, N.; Marrot, J.; Férey, G. *J. Am. Chem. Soc.* **2005**, *127*, 12788. (c) Sudik, A. C.; Côté, A. P.; Yaghi, O. M. *Inorg. Chem.* **2005**, *44*, 2998. (d) Wang, Z.; Zhang, B.; Inoue, K.; Fujiwara, H.; Otsuka, T.; Kobayashi, H.; Kurmoo, M. *Inorg. Chem.* **2007**, *46*, 437. (e) Yang, G.; Raptis, R. G. *Chem. Commun.* **2004**, 2058. (f) Yoon, J. H.; Choi, S. B.; Oh, Y. J.; Seo, M. J.; Jhon, Y. H.; Lee, T.-B.; Kim, D.; Choi, S. H.; Kim, J. *Catal. Today* **2007**, *120*, 324.
(25) (a) Friedrichs, O. D.; O'Keeffe, M.; Yaghi, O. M. *Acta Crystallogr.* **2003**, *A59*, 22. (b) Luo, T.-T.; Tsai, H.-L.; Yang, S.-L.; Liu, Y.-H.; Yadav, R. D.; Su, C.-C.; Ueng, C.-H.; Lin, L.-G.; Lu, K.-L. *Angew. Chem., Int. Ed.* **2005**, *44*, 6063. (c) Perman, J. A.; Dubois, K.; Nouar, F.; Zoccali, S.; Wojtas, y.; Eddaoudi, M.; Larsen, R. W.; Zaworotko, M. J. *Cryst. Growth Des.* **2009**, *9*, 5021. (d) Eckhardt, R.; Hanika-Heidl, H.; Fischer, R. D. *Chem.—Eur. J.* **2003**, *9*, 1795. (e) Lu, J.; Harrison, W T. A.; Jacobson, A. J. *Angew. Chem., Int. Ed.* **1995**, *34*, 2557. (f) Hao, H.-Q.; Wang, J.; Liu, W.-T.; Tong, M.-L. *CrystEngComm* **2008**, *10*, 1454.
(26) The specific pore volume of the adsorbent was estimated from the adsorption isotherm assuming that the density of the adsorbate in the pore at a given temperature and at its saturation pressure is the same as that of the adsorbate in its liquid state at the given temperature.
(27) Zhao, D.; Yuan, D.; Zhou, H.-C. *Energy Environ. Sci.* **2008**, *1*, 222.
(28) (a) Cole, J. H.; Everett, D. H.; Marshall, C. T.; Paniego, A. R.; Powl, J. C.; Rodriguez-Reinoso, F. *J. Chem. Soc., Faraday Trans.* **1974**, *70*, 2154. (b) O'Koye, I. P.; Benham, M.; Thomas, K. M. *Langmuir* **1997**, *13*, 4054.